Author Manuscript

Author Manuscript

Author Manuscript

Author Manuscript

HHS Public Access

Author manuscript

J Cardiovasc Pharmacol. Author manuscript; available in PMC 2017 May 01.

Published in final edited form as:

J Cardiovasc Pharmacol. 2016 May ; 67(5): 433–441. doi:10.1097/FJC.0000000000000369.

Potential Role of Axonal Chemorepellent Slit2 in Modulating Adventitial Inflammation in a Rat Carotid Artery Balloon Injury Model

Dong Liu, PhD[1], **Yan Xiao, MD**[1], **Romesh R. Subramanian, PhD**[2], **Ei-ichi Okamoto, MD**[2], **Josiah N. Wilcox, PhD**[2], **Leonard Anderson, PhD**[1], and **Hector De Leon, MD, PhD**[1]

[1]Cardiovascular Research Institute, Morehouse School of Medicine, Atlanta, GA 30310

[2]The Winship Cancer Institute, Emory University School of Medicine, Atlanta GA 30322

Abstract

Leukocyte infiltration of adventitial and perivascular tissues is an early event in the development of vascular remodeling after injury. We investigated whether Slit/Robo—an axonal chemorepellent system in vertebrate and invertebrate development—is activated during the inflammatory phase that follows endothelial denudation. Using the rat carotid artery model of angioplasty, we conducted a time course analysis of mRNAs encoding Slit ligands (Slit2 and Slit3) and Robo receptors (Robo1, Robo2 and Robo4), as well as proinflammatory cell adhesion molecule (CAM) genes. Adventitial inflammatory cells were counted in immunostained arterial sections. E-selectin, vascular CAM-1 (VCAM-1), and intercellular CAM-1 (ICAM-1) were upregulated 2–3 hr after injury, followed by infiltration of neutrophils and monocytes as evidenced by real-time PCR, in situ hybridization, and immunohistochemistry. Slit2, Slit3, and Robo genes exhibited no expression changes at 3 hr; however, they were markedly upregulated 1 day after angioplasty. ICAM-1 expression was reduced by 50%, and the number of adventitial neutrophils decreased by >75% one day after angioplasty. Slit2 has been shown to be a potent chemorepelent of leukocytes, endothelial cells and smooth muscle cells. Thus, we decided to further investigate the localization of Slit2 in injured vessels. Immunohistochemical stainings revealed the presence of Slit2 within the vessel wall and in the perivascular vasa vasorum of naive and injured arteries. Double immunohistochemical analyses showed that infiltrating monocytes expressed Slit2 in the perivascular and adventitial tissues of injured arteries 1 and 3 days postangioplasty. In addition, recombinant full-length Slit2 and Slit2-N/1118, an N-terminal fragment of Slit2, inhibited stromal cell-derived factor 1 (SDF-1)-mediated migration of circulating rat peripheral blood mononuclear cells. In summary, adventitial activation of CAM genes and neutrophil infiltration preceded upregulation of Slit/Robo genes. Sli2 expression colocalized with infiltrating inflammatory cells in the adventitial layer. This temporospatial association suggests that leukocyte chemorepellent Slit2 may be involved in halting the adventitial accumulation of inflammatory cells in injured vessels.

Corresponding authors: Hector De Leon, MD, PhD, DSP, Rue de la Chapelle 26, Peseux, NE, Switzerland, Tel: +41 79 175 9481, hdeleon68@hotmail.com. Dong Liu, MD, PhD. 720 Westview Drive SW. Atlanta, GA 30310. Tel: (404) 756 8916. dliu@msm.edu.

Conflict of Interest

The authors have no conflicts of interest to disclose.

Author Manuscript Author Manuscript Author Manuscript Author Manuscript

Keywords

Chemorepulsion; Cell Migration; Slit2; Robo Receptors; Adventitial Inflammation; Vascular Injury

1. Introduction

Inflammatory responses characterized by migration of leukocytes into injured vessels require cytokine-induced expression of cell adhesion molecules (CAMs).[1–3] CAM expression on endothelial cells (ECs) at the leading edge of the regenerating endothelium and on macrophages infiltrating the developing neointima are well-documented events.[4–6] In addition to luminal recruitment of inflammatory cells, balloon angioplasty of pig coronary arteries results in extensive activation of ECs in the perivascular vasa vasorum with subsequent recruitment of inflammatory cells into the adventitia and perivascular tissues.[7] The association of human coronary atherogenesis and adventitial inflammation,[8] and data indicating that perivascular adipose tissue plays a role in vascular function and disease[9] have triggered a renewed interest in the migratory behavior of leukocytes that infiltrate the perivascular space. Attraction and positioning of resident and inflammatory cells within the arterial layers take place following various migration pathways: media to lumen migration (e.g. VSMCs),[10] accumulation of circulating cells in the intima (e.g. monocytes/macrophages),[4–6] and adventitial entry of leukocytes (e.g. neutrophils, macrophages).[7] These studies, and an extensive body of research on the chemotactic arm of cell migration, have led to key advances in our understanding of the cellular and molecular events involved in arterial cell and leukocyte chemoattraction.[11–13] However, the contribution of chemorepulsive factors to halting of the inflammatory process that ensues following arterial injury remains largely unexplored.

We have demonstrated that Slit2/Robo, a ligand-receptor chemorepellent system described in models of axonal migration and leukocyte chemotaxis,[14–16] is also expressed in intact arteries and prevents PDGF-mediated migration of human VSMC.[17] Slit2 is proteolytically cleaved into Slit2-N and Slit2-C fragments. Slit2-N binds to Robo, a single-pass transmembrane receptor.[18, 19] Our previous data indicated that in addition to ECs, cells present in adventitial tissue of large vessels also expressed Slit2.[17] This finding triggered our interest to further investigate whether adventitial expression of Slit2 was regulated in response to mechanical endothelial denudation. Here, we report that upregulation of expression of mRNAs encoding Slit2 and Robo genes is subsequent to activation of inflammatory CAM genes and recruitment of neutrophils to the adventitial injury site. Slit2 protein was immunolocalized in adventitial resident and inflammatory cells, and recombinant full-length Slit2 and Slit2-N inhibited SDF-1-induced migration of leukocytes. We postulate that locally secreted Slit2 may contribute to halting of the extensive inflammatory responses evoked by mechanical injury or by atherosclerotic plaque development in large arteries.

Author Manuscript Author Manuscript Author Manuscript Author Manuscript

2. Methods

Rat Common Carotid Artery Balloon Injury Model

Animal studies were approved by the Institutional Animal Care and Use Committees of the Atlanta University Center and Emory University, and conformed to the NIH guidelines (Guide for the care and use of laboratory animals). We performed balloon injury of the common carotid artery as previously described.[20] Briefly, male Sprague-Dawley rats (350–400 g) were anesthetized with an intraperitoneal injection of ketamine (150 mg/kg) and xylazine (20 mg/kg). A Fogarty 2F balloon embolectomy catheter was introduced through the right femoral artery and advanced into the aorta and left common carotid artery until its bifurcation. The balloon was then inflated and withdrawn to the proximal end of the common carotid artery. This procedure was repeated 3 times. Carotid arteries from treatment-naive animals were used as controls.

Tissue Harvesting and Processing

Rats were euthanized with CO2 and thoracotomies performed as previously described.[17] The left ventricle was cannulated, the right atrium cut open, and the animals were perfused with PBS. Left common carotid arteries from balloon-injured animals, and thoracic aortas, common carotid arteries and brains from treatment-naive rats were collected for RNA extraction and immunohistochemical assays. Vascular and brain tissues were quickly harvested, placed in RNA*later* (Ambion, Austin, TX), snap-frozen in liquid nitrogen and stored at −80°C for further processing. Common carotid arteries from a separate group of balloon-injured animals were collected for immunohistochemistry at 2 hr, 1, 3, and 30 days (n=3 per group) after angioplasty. Arteries were harvested and fixed in 2% paraformaldehyde for 3 hours at 4°C, transferred to 15% sucrose overnight for cryoprotection, and embedded in Tissue-Tek O.C.T. compound (EMS, Hatfield, PA). Tissue blocks were frozen in liquid nitrogen, stored at −80°C and 6-μm thick sections obtained.

Real-Time PCR Analysis

Rat brain and vascular tissues were homogenized in lysis buffer (RLT, Qiagen) at 4°C using a Fast Prep homogenizer (Thermo Electron Corporation). Total RNA was isolated using RNeasy Mini Kits (Qiagen). RNA was reverse-transcribed with oligo-dT priming using the Advantage cDNA PCR kit (BD Biosciences, San Jose, CA). Primer sets used to amplify rat Slit ligands, Robo receptors and ICAM-1 are listed in Table 1. Relative quantitative real-time PCR was performed using the Roche LightCycler real-time thermal cycler (Roche Diagnostics). cDNA samples (100 ng each) were mixed with primers and the SYBR green Taq Ready Mix (Sigma, St. Louis, MO) for a total volume of 20 μl. Each gene was normalized to 18s (human/rat/mouse 18s, Lux primer set, Invitrogen) from the same sample. Amplified products were analyzed by electrophoresis on 2% agarose gels containing ethidium bromide (E-gels, Invitrogen) to confirm primer specificity. Rat β-actin (Lux primer set, Invitrogen) was amplified from the same cDNA samples for electrophoretic analysis.

Author Manuscript Author Manuscript Author Manuscript Author Manuscript

Immunohistochemistry

We performed immunohistochemical detection of Slit2 and leukocytes in vascular tissues using a goat polyclonal anti-human Slit2 antibody (Ab) (G-19, 1/200 dilution, Santa Cruz Biotechnology), and monoclonal anti-CD45 (clone OX-1, dilution 1/100, Pharmingen), Mononuclear Phagocyte (ED-1, clone 1C7, 1/100 dilution, Pharmingen), and anti-myeloperoxidase (MPO) (clone 2C7, 1/200 dilution, Serotec) antibodies. VSMCs were identified with an anti-smooth muscle α-actin (α-SMA) Ab (Clone 1A4, Sigma). Neutrophils (anti-MPO Ab), and monocytes (anti-ED-1 Ab) were detected in frozen sections using a biotinylated secondary antibody (goat anti-rabbit IgG at a 1/400 dilution or horse anti-mouse IgG at a 1/400 dilution; Vector Laboratories). This was followed by incubation with the avidin-biotin enzyme complex and chromogenic substrate (red reaction product) as described.[7] Serial sections treated with secondary antibodies (isotype IgG control) did not show any staining.

In Situ Hybridization

In situ hybridization methods utilized to detect E-selectin, VCAM, and MCP-1 using rat-specific ^{35}S-labeled riboprobes were performed as previously described.[21] Briefly, paraffin embedded, paraformaldehyde-fixed tissue sections were deparaffinized in xylene, rehydrated, washed in 0.5X SSC, pretreated with paraformaldehyde and proteinase K (Sigma) and prehybridized in 200 μL hybridization buffer (50% formamide; 0.3 mol/L NaCl; 20 mmol/L Tris, pH 8.0; 5 mmol/L EDTA; 0.02% polyvinylpyrrolidone; 0.02% Ficoll; 0.02% BSA; 10% dextran sulfate; and 10 mmol/L DTT) at 42°C. Serial sections were hybridized with 12X10^5 cpm of ^{35}S-labeled riboprobes at 55°C. After hybridization, the sections were washed in 2X SSC (1X SSC=150 mmol/L NaCl, 15 mmol/L sodium citrate, pH 7.0) with 10 mmol/L β-mercaptoethanol and 1 mmol/L EDTA, treated with RNase A (Sigma), and washed in the same buffer followed by a high-stringency wash in 0.1X SSC with 10 mmol/L β-mercaptoethanol and 1 mmol/L EDTA at 55°C. The slides were then washed in 0.5X SSC and dehydrated in graded alcohols containing 0.3 mol/L ammonium acetate. The sections were dried, coated with NTB2 nuclear track emulsion (International Biotechnologies), and exposed in the dark at 4°C for 8 to 12 weeks. After development, the sections were counterstained with hematoxylin and eosin to aid in cell identification.

Probes: Rat cDNA fragments encoding for E-selectin (475 bp) and VCAM-1 (581 bp) and MCP 1 were generated as reported elsewhere.[22–24] cDNA fragments encoding for rat P-selectin (675 bp), were amplified by reverse-transcriptase polymerase chain reaction (RT-PCR) from rat aorta treated with LPS (1 mg/mL) for 4 hours, and subcloned into pGEM3Z vectors (Promega). The following primer sequences were used for PCR amplification: rat P-selectin, 5′-TTTCACGCTGAGAGGAGCTGAC, 3′ GTTATCACTACTTGACGAGGTTGGG. The DNA sequence of these cDNAs was confirmed by sequencing.

Slit2 Expression Constructs

Full-length Slit2 (aminoacids [aa] 1-1529, MRGVGW to CTRCVS) and Slit2-N/1118 (aa 1-1118, MRGVGW to FSPPMV) were generated by cloning pDONR221/Slit2 and pDONR221/Slit2-N/1118 into pcDNA-DEST40 (Invitrogen) containing a V5/6xHis tag at

Author Manuscript Author Manuscript Author Manuscript Author Manuscript

the C-terminus as described elsewehre.[17]. The ViraPower Adenoviral Gateway expression system (Invitrogen) was used to generate Ad particles encoding Slit2 (Ad/Slit2/V5) and Slit2-N/1118 (Ad/Slit2-N/1118/V5) as previously reported.[17]

Peripheral blood mononuclear cell (PBMC) Migration Assay

Rat PBMCs were isolated by cell density gradients (Hystopaque 1083, Sigma). Blood was withdrawn from the right atrium of euthanized rats (see above) and collected in tubes containing EDTA. We incubated $4x10^4$ cells on standard cell migration inserts (5 μm pore size, Corning, Acton MA) in the presence and absence of purified Slit2 or Slit2-N/1118 added to the upper chamber, and stimulated with 10 ng/ml of SDF-1 (C-X-C motif ligand 12, CXCL12) (R&D Systems, Minneapolis, MN) added to the lower chambers. PBMCs were incubated at 37°C for 3 hours and cells that migrated to the lower chamber were counted by microcytometry and expressed as a percentage of the total number of cells placed on the insert. Three separate experiments (n=3 inserts per experiment) were conducted.

Statistics

Results are expressed as mean±SEM. Data were evaluated by t-tests or a one-way analysis of variance (ANOVA). When the overall F test of the ANOVA analysis was significant, a multiple comparison test (Tukey) was applied to identify the sources of differences. Differences were considered to be statistically significant when $P<0.05$.

3. Results

Slit/Robo Genes are Expressed in Rat Common Carotid Arteries and mRNA Expression is Upregulated after Balloon Injury

Real-time PCR products for all genes ran as single bands of the expected size and all genes were expressed in rat brain (Figure 1A). Slit2, Slit3, Robo1, Robo2 and Robo4 were expressed in rat carotid arteries, whereas Slit1 (Figure 1A) and Robo3 (not shown) expression levels were negligible in uninjured carotid arteries. Slit/Robo mRNA expression was quantified by real-time PCR relative to expression levels detected in rat brain of naive animals. Arterial injury resulted in a 21- and 3-fold increase in the expression levels of Slit2 and Slit3, respectively, at day 1 after injury (Figure 1C and D). Expression of Slit 2 and Slit3 was attenuated at 3, 7 and 30 days postinjury. Expression levels of Robo1, Robo2 and Robo4 receptors were upregulated 1 day after angioplasty by 10-, 15- and 5-fold, respectively (Figure 1E, F and G). Although expression levels of Robo1 and Robo2 remained higher than control at 3, 7 and 30 days after injury, differences were not statistically significant. Robo4 showed a biphasic upregulation effect at 1 and 30 days. ICAM-1 mRNA expression was increased 9-fold and 4-fold at 3 hr and 1 day postangioplasty, respectively (Figure 1H). No changes in expression levels were detected for any Slit/Robo gene at 3 hr postinjury. Mechanical injury did not modify either Slit1 (Figure 1A) or Robo3 (not shown) mRNA expression at any time point examined.

Author Manuscript Author Manuscript Author Manuscript Author Manuscript

Cells Expressing Slit2 Localize to Medial VSMCs and ECs of Large Vessels, and to the Adventitial Vasa Vasorum

Control uninjured vessels showed Slit2 positive ECs lining the lumen of the main vessel, as well as the luminal side of small and middle size vessels in the perivascular tissue (Figure 2A). Adventitial fibroblast-like cells and few medial cells were Slit2 positive in naive vessels. However, 1-day post-injury carotid arteries exhibited numerous inflammatory-like Slit2 positive cells in the adventitia (Figure 2B). The medial layer also showed an intense immunopositive staining at this time point. Thirty days after injury, a diffuse Slit2 positive staining was found in the neointimal and medial layers (Figure 2C). The endothelial lining of adventitial and perivascular arteries and arterioles were Slit2 positive at 30 days (Figure 2C).

Neutrophil and Macrophage Accumulate in the Adventitia of Injured Vessels Following Upregulation of Chemokine and CAM Expression

Normal carotid arteries stained with an anti-α-SMA Ab to identify the adventitial vasa vasorum showed the lumen of these vessels free of inflammatory cells (Figure 3A). As early as 2 hr after injury, the adventitial space surrounding the injury site was filled with MPO-positive neutrophils (Figure 3B). Accumulation of granulocytes was also evident in the adventitial space surrounding injured vessels as early as 1 day after angioplasty (Figure 3C). ED-1 positive monocyte/macrophages infiltrated the adventitia abundantly 3 days after angioplasty (Figure 3D). Neutrophils and monocytes were rarely detected on the luminal surface of the injured vessels at any time. In situ hybridization experiments detected EC expression of E-selectin, and VCAM-1 mRNAs in the adventitial vasa vasorum 2 hr after injury (Figure 3E and F). MCP-1 mRNA was abundantly expressed by adventitial cells at the same time point (Figure 3G). The highest number of neutrophils infiltrating the adventitial space was reached 6 hr after angioplasty and it declined rapidly, whereas the highest number of adventitial monocytes/macrophages was observed 3 days after injury (Figure 4). Neutrophils and monocytes/macrophages were reduced by more than 75% by days 1 and 5, respectively (Figure 4).

Infiltrating Monocytes and Granulocytes Colocalize with Adventitial Slit2-Expressing Cells in Balloon Injured Arteries

To further identify the cell types expressing Slit2 in the adventitia and perivascular space, double label immunohistochemistry of 1– and 3–day balloon–injured vessels was conducted using antibodies against Slit2 and CD45 (a panleukocyte marker); Slit2 and ED-1 (a monocyte/macrophage marker); and Slit2 and MPO (a marker of granulocytes). Slit2 was detected using a secondary Ab conjugated to a green fluorochrome (Alexa Fluor 488), whereas CD45, ED-1 and MPO positive cells were identified by a secondary Ab conjugated to a red fluorochrome (Alexa Fluor 594). Fluorescence microscopy revealed colocalization of CD45 positive cells expressing Slit2 in the perivascular and adventitial spaces 1 and 3 days after balloon angioplasty (Figure 5A and B). Colabeling of 1–day sections with anti-Slit2 and anti-MPO, and anti-Slit2 and anti-ED-1 antibodies revealed that Slit2-expressing cells were also positive for MPO and ED-1 (Figure 6A and B). Slides incubated with non-immune IgG showed no staining (Figure 5C and 6C).

Author Manuscript Author Manuscript Author Manuscript Author Manuscript

Identification of Full-Length Slit2 and Slit2-N/1118 in HEK-293 Cells

HEK-293 cells were infected with Ad/Slit2/V5, Ad/Slit2-N/1118/V5, and Ad/CMV/V5 (control) vectors. C-terminus V5-tagged Slit2 and Slit2-N/1118 were identified in conditioned media (CM) by Western blot analysis. Ad/Slit2/V5 rendered 2 proteins of approximately ~190 and ~55 kDa, corresponding to full-length Slit2 and Slit2-C (Figure 7A, lanes b). The cleaved N-terminal fragment of Slit2 (~140 kDa) was not detected in CM of cells infected with Ad/Slit2/V5 as only the C-terminal fragment remains tagged upon cleavage. Slit2-N/1118 (~140 kDa), our engineered construct, was found in CM from Ad/Slit2-N/1118/V5-infected cells (Figure 7A, lanes c), whereas no protein was detected in HEK-293 cells infected with Ad/CMV/V5 (Figure 7A, lane a).

Full-length Slit2 and Slit2-N/1118 Inhibit SDF-1-Induced Migration of Circulating PBMCs

Biological activity of Slit2 and Slit2-N/1118 was tested in a transwell migration assay using rat PBMCs. PBMCs were incubated for 3 hr in cell migration inserts (5 μm pore size) and 10 ng/ml of SDF-1 was added to the lower chambers in the presence and absence of CM from Ad/CMV/V5-, Ad/Slit2/V5- and Ad/Slit2-N/1118/V5-infected HEK 293 cells. SDF-1 induced a 3.4-fold increase in PBMC migration, and CM from HEK cells containing Slit2 and Slit2-N/1118 completely blocked SDF-1-induced PBMC migration, indicating that Slit2-N/1118 is a biologically active fragment (Figure 7B).

4. Discussion

In response to injury, resident arterial cells and inflammatory cells follow various migration pathways guided by locally produced chemoattractants. The resulting structural remodeling that generates intimal thickening and adventitial neovascularization and fibrosis is associated with an increased expression of inflammation-related molecules.[25, 26] The transient nature of the inflammatory response that occurs in the adventitia of injured vessels,[7] suggests that endogenous antichemotactic factors may participate in halting leukocyte infiltration and neointimal growth. In the present study, rat carotid arteries subjected to balloon angioplasty showed a time-dependent upregulation of mRNAs encoding Slit2, Slit3, Robo1, Robo2 and Robo4. ICAM-1, E-selectin, VCAM-1 and MCP-1 expression preceded the adventitial infiltration of neutrophils, and both events were followed by upregulation of Slit/Robo mRNAs. This temporal sequence of molecular and cellular events suggests that transcription of chemorepellent Slit/Robo genes may be activated in response to vascular inflammation. Although we found high vascular expression of Slit2 and Slit3 ligands, we decided to focus the present study on Slit2 to deepen our knowledge on a molecule that may have therapeutic potential to prevent vascular lesion formation.

In agreement with our working model, Slit2 has recently been shown to inhibit adhesion of monocytes to activated ECs and to immobilized ICAM-1 and VCAM-1.[27] At day 1 postinjury, when the highest levels of Slit/Robo were observed, ICAM-1 expression had already decreased by 50%, whereas the number of adventitial neutrophils was reduced by more than 75%. Our data showed a temporospatial relationship between expression of CAMs / MCP-1 and recruitment of inflammatory cells, and vascular expression of Slit/Robo, suggesting that antichemotactic molecules may be involved in halting the adventitial

Author Manuscript Author Manuscript Author Manuscript Author Manuscript

entry and trafficking of leukocytes. In agreement with this concept, systemic administration of Slit2 has been shown to reduce monocyte recruitment to atherosclerotic lesions in LDL receptor-deficient mice[27] and macrophage infiltration in rats with crescent glomerulonephritis.[28] Moreover, Slit2 administration to mice that underwent renal ischemia reperfusion injury resulted in inhibition of neutrophil and macrophage infiltration.[29] It has recently been reported that Slit2-Robo4 signaling is involved in the regulation of LPS-induced endothelial inflammation. LPS enhanced endothelial inflammation by downregulating the expression of Slit2 and Robo4.[30] The anti-inflammatory actions of Slit2 have been recently expanded to include crucial biological effects on platelets. Slit2 has been shown to be a negative regulator of platelet function and to prevent the formation of stable occlusive thrombi.[31]

Double-label immunohistochemistry revealed that adventitial monocytes/macrophages expressed Slit2 three days after injury. As previously reported by Wu et al,[16] we have found no Slit2 expression in rat PBMCs (not shown); therefore, Slit2 expression by macrophages is likely activated upon entry of monocytes to the adventitial tissue. Additional studies are warranted to screen for molecular activators of Slit2 in PBMCs. Robo4 has been reported to be preferentially expressed by ECs, and Slit2 prevents VEGF-mediated migration of ECs.[32] In the current study, Robo4 expression exhibited a biphasic upregulation at days 1 and 30 postangioplasty. Upregulation of Robo4 at day 1 may be driven by the acute adventitial inflammatory response and the increased expression of CAMs in this layer. However, adventitial inflammation subsides within the first week after injury rendering it an unlikely candidate to regulate Robo4 expression at 30 days. Thus, we hypothesize that the upregulation of Robo4 observed at 30 days postinjury is related to the reendothelialization process taking place at this time.[33, 34] Slit2 mRNA expression levels returned to control values at day 30, whereas a diffuse immunopositive Slit2 staining was still present throughout the neointima and media layers. Sustained expression of Slit2 protein in the neointima 30 days after injury in the absence of significantly upregulated levels of Slit2 mRNA may be accounted for by a longer protein half-life. The intima and media layers are not major sites of localization of inflammatory cells since few leukocytes are found in these regions at any time after injury.[7, 35] Thus, we speculate that the functional significance of Slit2 secreted by neointimal cells may reside in modulating cell positioning during intimal thickening development.

Slit2-N binds the extracellular domain of Robo and this fragment is responsible for axonal migration and branching.[36, 37] Our functional analysis suggests that recombinant full-length Slit2 and Slit2-N have similar properties in PBMCs.[17] Whether Slit2-N/1118 is an endogenously cleaved product within the vessel wall is unknown. In a separate study, we have shown that Slit2-N/1118 also inhibits PDGF-mediated migration of VSMCs by preventing the activation of small Rho GTPase Rac1.[17] In keeping with the role of PDGF in VSMC migration, Slit2 may modulate the effects of promigratory molecules involved in attracting VSMCs to the neointimal mass, albeit the net outcome results in generation of a neointima layer. It remains to be determined whether Slit2-N/1118 retains its anti-inflammatory actions in vivo by preventing adventitial infiltration of immune cells and neointima formation. The lack of selectivity of Slit2 to bind Robo1 or Robo2[38] suggests that Slit2 may bind and activate several Robo receptors. Cell localization and predominance of

Author Manuscript Author Manuscript Author Manuscript Author Manuscript

Robo1, Robo2 and Robo4 receptors within the vessel wall will require additional studies. As for the cell source of Slit2 ligand in vivo, our data suggest that ECs and VSMCs, as well as inflammatory cells may secrete Slit2, which may then bind Robo receptors in a cell–to–cell or cell–independent manner. Using conditional knockout mice, Rama et al have recently shown that Slit2 is a potent promoter of retinal neovascularization through Robo1 and Robo2 receptors.[39] Whether Slit2 also participates in the adventitial neovascularization process observed in injured vessels remains to be investigated. The unique properties of Slit2 to selectively avert migration of leukocyte subpopulations to injured tissues, and its ability to impair platelet adhesion and spreading, places this molecule not only as a key regulator of vascular function but also as a novel therapeutic tool to prevent inflammation-driven vascular and renal injury.[27, 40, 41]

5. Conclusion

In conclusion, our data broadens the functional significance of Slit2 as a negative regulator of leukocyte migration in mechanically-injured vessels. The antichemotactic effects of Slit2 on VSMCs and inflammatory cells underline the importance of inhibitory signals involved in modulating vascular inflammation and arterial cell migration. Further studies aimed at silencing the expression of Slit2 in conditional Slit2 and Slit2-signalling knockout mice will allow us to define the role of Slit2 in vascular development and injury. These studies are also necessary to determine the potential therapeutic benefits of manipulating cell repulsion mechanisms in atherosclerotic arteries.

Acknowledgments

Funding

This work was supported in part by funding from the Georgia Tech/Emory Center (GTEC) for the Engineering of Living Tissues, an ERC Program of the National Science Foundation under Award Number EEC-9731643 and a grant from the National Institutes of Health (NIH/P50HL117929).

The MCP-1 probe was kindly supplied by W. R. Taylor (Emory University, Atlanta, GA).

References

1. Gimbrone MA Jr, Garcia-Cardena G. Vascular endothelium, hemodynamics, and the pathobiology of atherosclerosis. Cardiovasc Pathol. 2013 Jan-Feb;22(1):9–15. [PubMed: 22818581]
2. Marx N, Sukhova GK, Collins T, Libby P, Plutzky J. PPARalpha activators inhibit cytokine-induced vascular cell adhesion molecule-1 expression in human endothelial cells. Circulation. 1999 Jun 22; 99(24):3125–31. [PubMed: 10377075]
3. Springer TA. Traffic signals for lymphocyte recirculation and leukocyte emigration: the multistep paradigm. Cell. 1994 Jan 28; 76(2):301–14. [PubMed: 7507411]
4. Landry DB, Couper LL, Bryant SR, Lindner V. Activation of the NF-kappa B and I kappa B system in smooth muscle cells after rat arterial injury. Induction of vascular cell adhesion molecule-1 and monocyte chemoattractant protein-1. Am J Pathol. 1997 Oct; 151(4):1085–95. [PubMed: 9327742]
5. Roque M, Fallon JT, Badimon JJ, Zhang WX, Taubman MB, Reis ED. Mouse model of femoral artery denudation injury associated with the rapid accumulation of adhesion molecules on the luminal surface and recruitment of neutrophils. Arterioscler Thromb Vasc Biol. 2000 Feb; 20(2): 335–42. [PubMed: 10669628]

Author Manuscript Author Manuscript Author Manuscript Author Manuscript

6. Verheyen AK, Vlaminckx EM, Lauwers FM, Saint-Guillain ML, Borgers MJ. Identification of macrophages in intimal thickening of rat carotid arteries by cytochemical localization of purine nucleoside phosphorylase. Arteriosclerosis. 1988 Nov-Dec;8(6):759–67. [PubMed: 3143345]
7. Okamoto E, Couse T, De Leon H, Vinten-Johansen J, Goodman RB, Scott NA, Wilcox JN. Perivascular inflammation after balloon angioplasty of porcine coronary arteries. Circulation. 2001 Oct 30; 104(18):2228–35. [PubMed: 11684636]
8. Kortelainen ML, Porvari K. Adventitial macrophage and lymphocyte accumulation accompanying early stages of human coronary atherogenesis. Cardiovasc Pathol. 2014 Jul-Aug;23(4):193–7. [PubMed: 24685316]
9. Brown NK, Zhou Z, Zhang J, Zeng R, Wu J, Eitzman DT, Chen YE, Chang L. Perivascular adipose tissue in vascular function and disease: a review of current research and animal models. Arterioscler Thromb Vasc Biol. 2014 Aug; 34(8):1621–30. [PubMed: 24833795]
10. Jackson CL, Raines EW, Ross R, Reidy MA. Role of endogenous platelet-derived growth factor in arterial smooth muscle cell migration after balloon catheter injury. Arterioscler Thromb. 1993 Aug; 13(8):1218–26. [PubMed: 8343497]
11. Ikari Y, Yee KO, Schwartz SM. Role of alpha5beta1 and alphavbeta3 integrins on smooth muscle cell spreading and migration in fibrin gels. Thromb Haemost. 2000 Oct; 84(4):701–5. [PubMed: 11057873]
12. Ohno N, Ichikawa H, Coe L, Kvietys PR, Granger DN, Alexander JS. Soluble selectins and ICAM-1 modulate neutrophil-endothelial adhesion and diapedesis in vitro. Inflammation. 1997 Jun; 21(3):313–24. [PubMed: 9246573]
13. Sallusto F, Baggiolini M. Chemokines and leukocyte traffic. Nat Immunol. 2008 Sep; 9(9):949–52. [PubMed: 18711431]
14. Nguyen Ba-Charvet KT, Brose K, Marillat V, Kidd T, Goodman CS, Tessier-Lavigne M, Sotelo C, Chedotal A. Slit2-Mediated chemorepulsion and collapse of developing forebrain axons. Neuron. 1999 Mar; 22(3):463–73. [PubMed: 10197527]
15. Ringstedt T, Braisted JE, Brose K, Kidd T, Goodman C, Tessier-Lavigne M, O'Leary DD. Slit inhibition of retinal axon growth and its role in retinal axon pathfinding and innervation patterns in the diencephalon. J Neurosci. 2000 Jul 1; 20(13):4983–91. [PubMed: 10864956]
16. Wu JY, Feng L, Park HT, Havlioglu N, Wen L, Tang H, Bacon KB, Jiang Z, Zhang X, Rao Y. The neuronal repellent Slit inhibits leukocyte chemotaxis induced by chemotactic factors. Nature. 2001 Apr 19; 410(6831):948–52. [PubMed: 11309622]
17. Liu D, Hou J, Hu X, Wang X, Xiao Y, Mou Y, De Leon H. Neuronal chemorepellent Slit2 inhibits vascular smooth muscle cell migration by suppressing small GTPase Rac1 activation. Circ Res. 2006 Mar 3; 98(4):480–9. [PubMed: 16439689]
18. Battye R, Stevens A, Perry RL, Jacobs JR. Repellent signaling by Slit requires the leucine-rich repeats. J Neurosci. 2001 Jun 15; 21(12):4290–8. [PubMed: 11404414]
19. Zallen JA, Yi BA, Bargmann CI. The conserved immunoglobulin superfamily member SAX-3/Robo directs multiple aspects of axon guidance in C. elegans. Cell. 1998 Jan 23; 92(2):217–27. [PubMed: 9458046]
20. De Leon H, Ollerenshaw JD, Griendling KK, Wilcox JN. Adventitial cells do not contribute to neointimal mass after balloon angioplasty of the rat common carotid artery. Circulation. 2001 Oct 2; 104(14):1591–3. [PubMed: 11581133]
21. De Leon H, Scott NA, Martin F, Simonet L, Bernstein KE, Wilcox JN. Expression of nonmuscle myosin heavy chain-B isoform in the vessel wall of porcine coronary arteries after balloon angioplasty. Circ Res. 1997 Apr; 80(4):514–9. [PubMed: 9118482]
22. Fries JW, Williams AJ, Atkins RC, Newman W, Lipscomb MF, Collins T. Expression of VCAM-1 and E-selectin in an in vivo model of endothelial activation. Am J Pathol. 1993 Sep; 143(3):725–37. [PubMed: 7689792]
23. Williams AJ, Atkins RC, Fries JW, Gimbrone MA Jr, Cybulsky MI, Collins T. Nucleotide sequence of rat vascular cell adhesion molecule-1 cDNA. Biochim Biophys Acta. 1992 Jun 15; 1131(2): 214–6. [PubMed: 1377031]

Author Manuscript Author Manuscript Author Manuscript Author Manuscript

24. Capers, Qt; Alexander, RW.; Lou, P.; De Leon, H.; Wilcox, JN.; Ishizaka, N.; Howard, AB.; Taylor, WR. Monocyte chemoattractant protein-1 expression in aortic tissues of hypertensive rats. Hypertension. 1997 Dec; 30(6):1397–402. [PubMed: 9403559]
25. Korshunov VA, Nikonenko TA, Tkachuk VA, Brooks A, Berk BC. Interleukin-18 and macrophage migration inhibitory factor are associated with increased carotid intima-media thickening. Arterioscler Thromb Vasc Biol. 2006 Feb; 26(2):295–300. [PubMed: 16293799]
26. Zhan Y, Brown C, Maynard E, Anshelevich A, Ni W, Ho IC, Oettgen P. Ets-1 is a critical regulator of Ang II-mediated vascular inflammation and remodeling. J Clin Invest. 2005 Sep; 115(9):2508–16. [PubMed: 16138193]
27. Mukovozov I, Huang YW, Zhang Q, Liu GY, Siu A, Sokolskyy Y, Patel S, Hyduk SJ, Kutryk MJ, Cybulsky MI, Robinson LA. The Neurorepellent Slit2 Inhibits Postadhesion Stabilization of Monocytes Tethered to Vascular Endothelial Cells. J Immunol. 2015 Aug 21.
28. Kanellis J, Garcia GE, Li P, Parra G, Wilson CB, Rao Y, Han S, Smith CW, Johnson RJ, Wu JY, Feng L. Modulation of inflammation by slit protein in vivo in experimental crescentic glomerulonephritis. Am J Pathol. 2004 Jul; 165(1):341–52. [PubMed: 15215188]
29. Chaturvedi S, Yuen DA, Bajwa A, Huang YW, Sokollik C, Huang L, Lam GY, Tole S, Liu GY, Pan J, Chan L, Sokolskyy Y, Puthia M, Godaly G, John R, Wang C, Lee WL, Brumell JH, Okusa MD, Robinson LA. Slit2 prevents neutrophil recruitment and renal ischemia-reperfusion injury. J Am Soc Nephrol. 2013 Jul; 24(8):1274–87. [PubMed: 23766538]
30. Zhao H, Anand AR, Ganju RK. Slit2-Robo4 pathway modulates lipopolysaccharide-induced endothelial inflammation and its expression is dysregulated during endotoxemia. J Immunol. 2014 Jan 1; 192(1):385–93. [PubMed: 24272999]
31. Patel S, Huang YW, Reheman A, Pluthero FG, Chaturvedi S, Mukovozov IM, Tole S, Liu GY, Li L, Durocher Y, Ni H, Kahr WH, Robinson LA. The cell motility modulator Slit2 is a potent inhibitor of platelet function. Circulation. 2012 Sep 11; 126(11):1385–95. [PubMed: 22865890]
32. Park KW, Morrison CM, Sorensen LK, Jones CA, Rao Y, Chien CB, Wu JY, Urness LD, Li DY. Robo4 is a vascular-specific receptor that inhibits endothelial migration. Dev Biol. 2003 Sep 1; 261(1):251–67. [PubMed: 12941633]
33. Kong D, Melo LG, Gnecchi M, Zhang L, Mostoslavsky G, Liew CC, Pratt RE, Dzau VJ. Cytokine-induced mobilization of circulating endothelial progenitor cells enhances repair of injured arteries. Circulation. 2004 Oct 5; 110(14):2039–46. [PubMed: 15451799]
34. Tsurumi Y, Murohara T, Krasinski K, Chen D, Witzenbichler B, Kearney M, Couffinhal T, Isner JM. Reciprocal relation between VEGF and NO in the regulation of endothelial integrity. Nat Med. 1997 Aug; 3(8):879–86. [PubMed: 9256279]
35. Hay C, Micko C, Prescott MF, Liau G, Robinson K, De Leon H. Differential Cell Cycle Progression Patterns of Infiltrating Leukocytes and Resident Cells After Balloon Injury of the Rat Carotid Artery. Arterioscler Thromb Vasc Biol. 2001; 21(12):1948–54. [PubMed: 11742869]
36. Chen JH, Wen L, Dupuis S, Wu JY, Rao Y. The N-terminal leucine-rich regions in Slit are sufficient to repel olfactory bulb axons and subventricular zone neurons. J Neurosci. 2001 Mar 1; 21(5):1548–56. [PubMed: 11222645]
37. Nguyen Ba-Charvet KT, Brose K, Ma L, Wang KH, Marillat V, Sotelo C, Tessier-Lavigne M, Chedotal A. Diversity and specificity of actions of Slit2 proteolytic fragments in axon guidance. J Neurosci. 2001 Jun 15; 21(12):4281–9. [PubMed: 11404413]
38. Brose K, Bland KS, Wang KH, Arnott D, Henzel W, Goodman CS, Tessier-Lavigne M, Kidd T. Slit proteins bind Robo receptors and have an evolutionarily conserved role in repulsive axon guidance. Cell. 1999 Mar 19; 96(6):795–806. [PubMed: 10102268]
39. Rama N, Dubrac A, Mathivet T, Ni Charthaigh RA, Genet G, Cristofaro B, Pibouin-Fragner L, Ma L, Eichmann A, Chedotal A. Slit2 signaling through Robo1 and Robo2 is required for retinal neovascularization. Nat Med. 2015 May; 21(5):483–91. [PubMed: 25894826]
40. Yuen DA, Robinson LA. Slit2-Robo signaling: a novel regulator of vascular injury. Curr Opin Nephrol Hypertens. 2013 Jul; 22(4):445–51. [PubMed: 23736842]
41. Chaturvedi S, Robinson LA. Slit2-Robo signaling in inflammation and kidney injury. Pediatr Nephrol. 2014 Apr 29.

Author Manuscript Author Manuscript Author Manuscript Author Manuscript

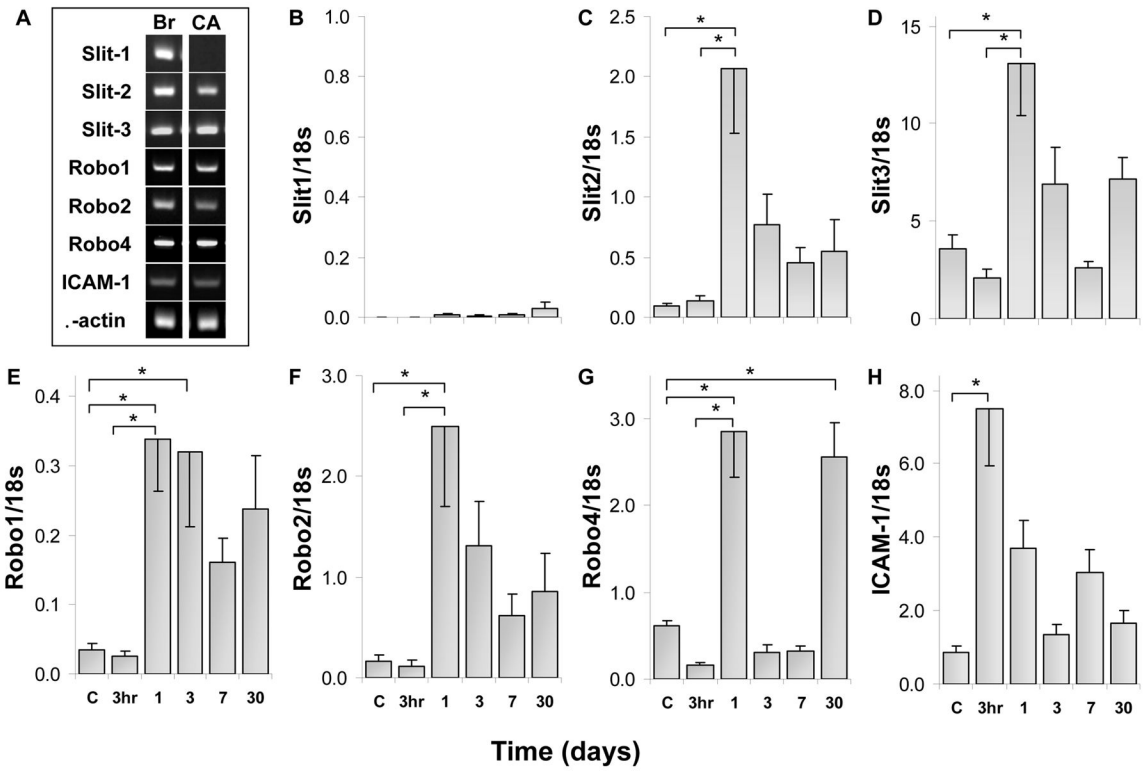

Figure 1. Time-dependant expression regulation of mRNAs encoding Slit/Robo genes in balloon angioplastied rat carotid arteries

A. Real-Time PCR products in rat brains (Br) and carotid arteries (CA). mRNA expression levels of Slit1 (B), Slit2 (C), Slit3 (D), Robo1 (E), Robo2 (F), and Robo4 (G) genes normalized to 18s were upregulated 1 day after angioplasty. Values represent mean±SEM of 6 injured or naive control (C) arteries obtained from independent animals. * $P<0.001$.

Author Manuscript Author Manuscript Author Manuscript Author Manuscript

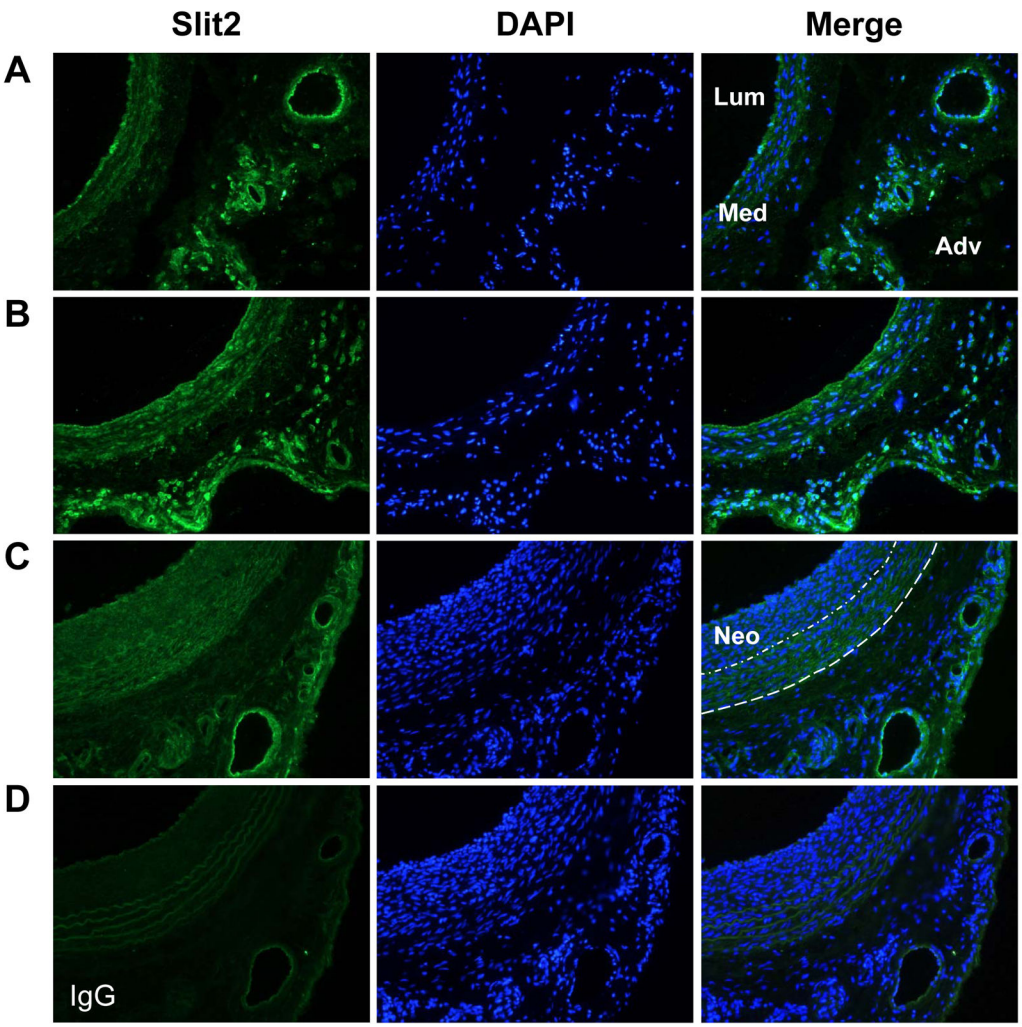

Figure 2. Immunohistochemical localization of Slit2 in balloon angioplastied rat common carotid arteries

Sections were incubated with an anti-Slit2 Ab and a secondary Ab conjugated to Alexa Fluor 488 (green). Slides were stained with DAPI (blue), and fluorescence images merged. **A:** Naive rat common carotid artery. The endothelial lining and media layer of the main vessel, as well as the adventitial vasa vasorum stained positive for Slit2. **B:** One-day injured arteries showed Slit2-positive medial and adventitial cells. **C:** Thirty-day injured carotid artery. A diffuse Slit2-positive staining was found in the neointima at 30 days; medial cells and adventitial vasa vasorum were also Slit2 positive. **D:** An unrelated IgG isotype was used as a negative control in a 30–day section; arterial autofluorescence was minimal. Lum: lumen; Med: media; Adv: adventitia, Neo: neointima. Dotted line: internal elastic lamina; interrupted line: external elastic lamina. Magnification: x200.

Author Manuscript Author Manuscript Author Manuscript Author Manuscript

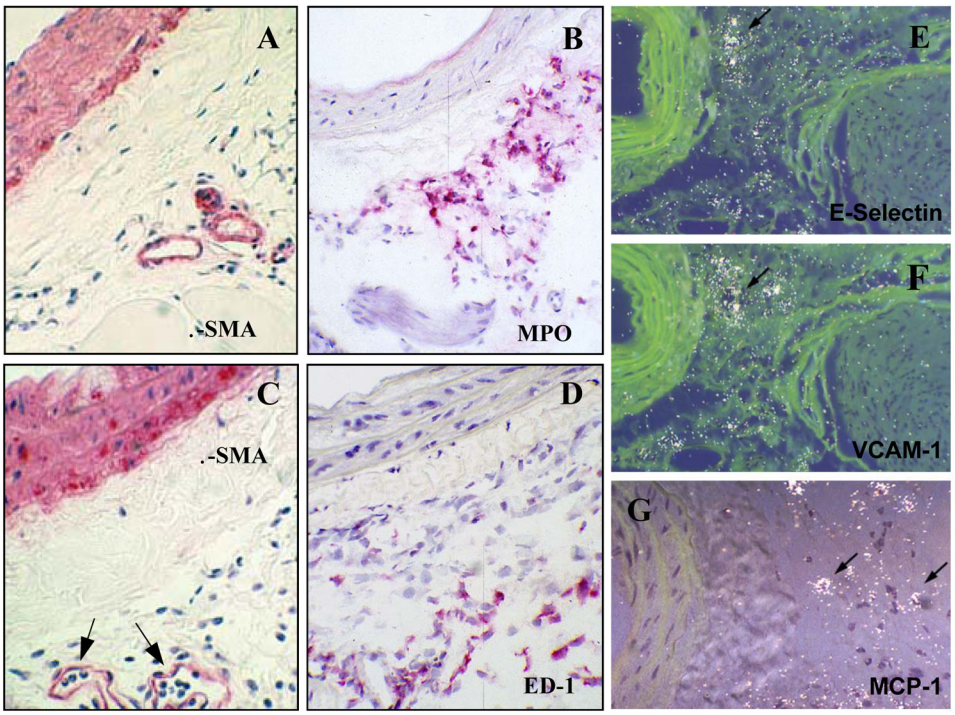

Figure 3. Morphological and Immunohistochemical Localization of Inflammatory Cells in Injured Vessels

VSMCs were identified with an anti-α-SMA Ab in frozen sections of naive (**A**) and 1–day injured (**C**) rat common carotid arteries. Neutrophils, detected by MPO staining, accumulated in the adventitia 2 hr after injury (**B**); whereas no MPO positive cells were found in naive arteries (not shown). Granulocytes and mononuclear inflammatory cells were found filling the lumen of adventitial veins 1 day after injury (**C**, arrows). VSMCs from adventitial arterioles (**A**) and veins (**C**) stained positive for α-SMA. **D**. ED-1 positive cells in the adventitia 3 days after angioplasty. **E–F**. Localization of CAMs and MCP-1 mRNAs by in situ hybridization. E-selectin (**E**), VCAM-1 (**F**), and MCP-1 (**G**) mRNAs were detected in the adventitial vasa vasorum and were absent on the luminal surface of the denuded vessels 2 hours after injury. In situ hybridizations shown were exposed for 12 weeks prior to development and staining with H&E. Magnification: x250.

Author Manuscript Author Manuscript Author Manuscript Author Manuscript

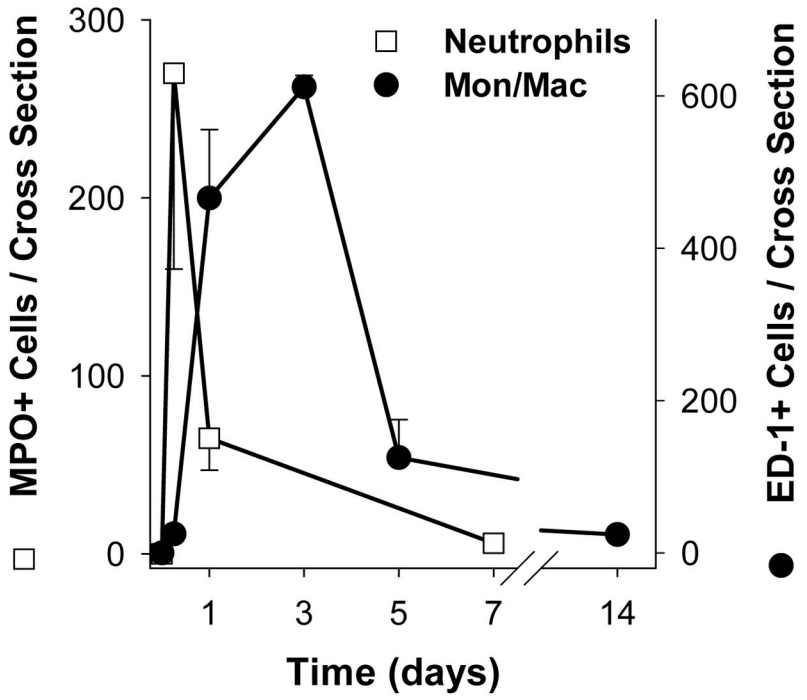

Figure 4. Time course analysis of the number of leukocytes accumulated in the adventitia

Adventitial neutrophils and monocytes/macrophages were counted in 3 to 4 arterial sections per artery immunostained with anti-MPO and anti-ED-1 Abs. Positive cells were counted by computer based image analysis.[7] The results were expressed as the total number of positive cells per vessel cross section (n=3 rats per time point). The number of neutrophils detected by MPO staining peaked at 6 hours, whereas the highest number of adventitial macrophages was observed 3 days after injury. Data are expressed as means±SEM.

Author Manuscript Author Manuscript Author Manuscript Author Manuscript

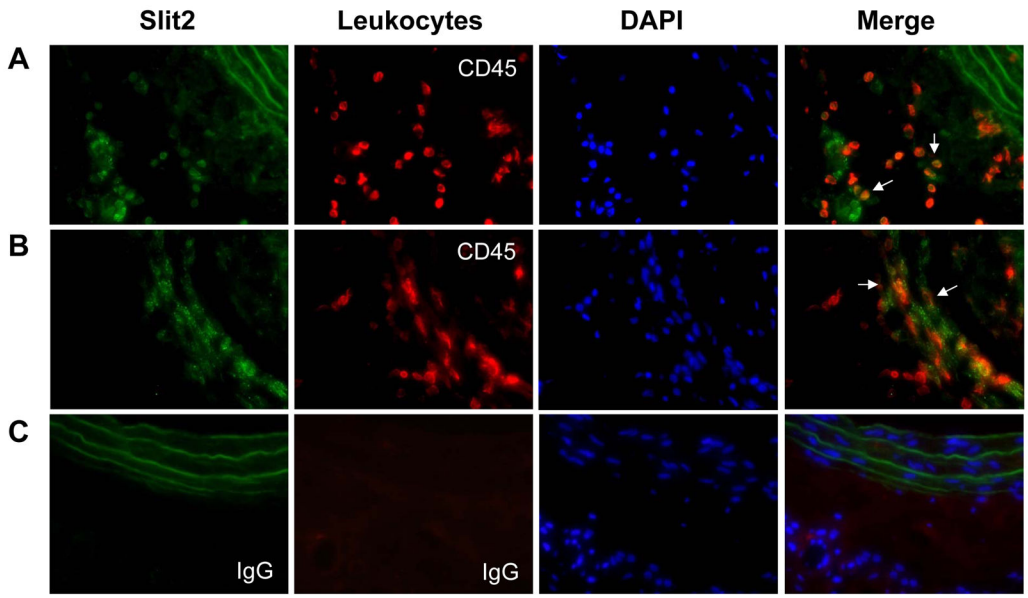

Figure 5. Immunohistochemical colocalization of Slit2 and inflammatory cells in the adventitia of injured rat carotid arteries

A: Double immunostaining with Abs directed against Slit2 and CD45 in a 1–day injured artery. **B:** Double labeling as in A in a 3–day injured vessel. **C:** One-day sections were stained with a non-immune IgG. Slides were labeled with a secondary Ab conjugated to Alexa Fluor 488 (green) to detect Slit2, whereas CD45 was detected with an Ab conjugated to Alexa Fluor 594 (red). Slides were stained with DAPI (blue) and fluorescence images captured and merged. Numerous CD45/Slit2 positive inflammatory cells were detected in the adventitial layer at days 1 (A) and 3 (B) after angioplasty (arrows). To better visualize Slit2/CD45 positive cells, DAPI images in A and B were not merged with Slit2 and CD45. Magnification: x400.

Author Manuscript Author Manuscript Author Manuscript Author Manuscript

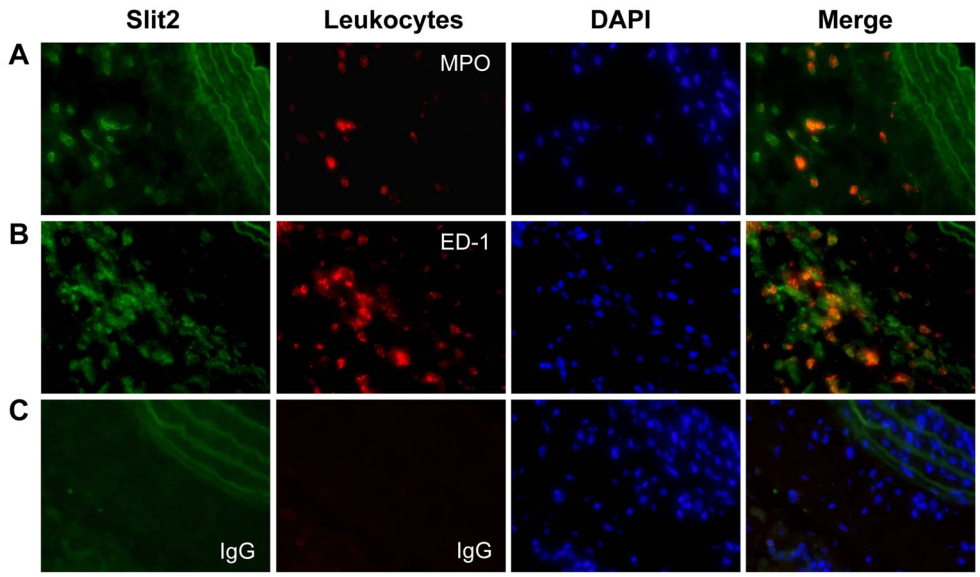

Figure 6. Immunohistochemical colocalization of Slit2 and MPO, and Slit2 and ED-1 in the adventitia of injured rat carotid arteries

A: Double immunostaining with Abs directed against Slit2 and MPO, a granulocyte marker, in a 1–day injured artery. **B:** Double labeling with Slit2 and ED-1, a monocyte/macrophage marker, in a 3–day injured vessel. **C:** One-day sections were stained with non-immune IgG. Slides were immunostained as described in Fig. 5. MPO and ED-1 were detected with an Ab conjugated to Alexa Fluor 594 (red). Slit2/MPO and Slit2/ED-1 positive cells were detected in the adventitial layer of 1– (A) and 3–day (B) injured vessels, respectively. To better visualize fluorescently-labeled cells, DAPI images in A and B were not merged. Magnification: x400.

Author Manuscript Author Manuscript Author Manuscript Author Manuscript

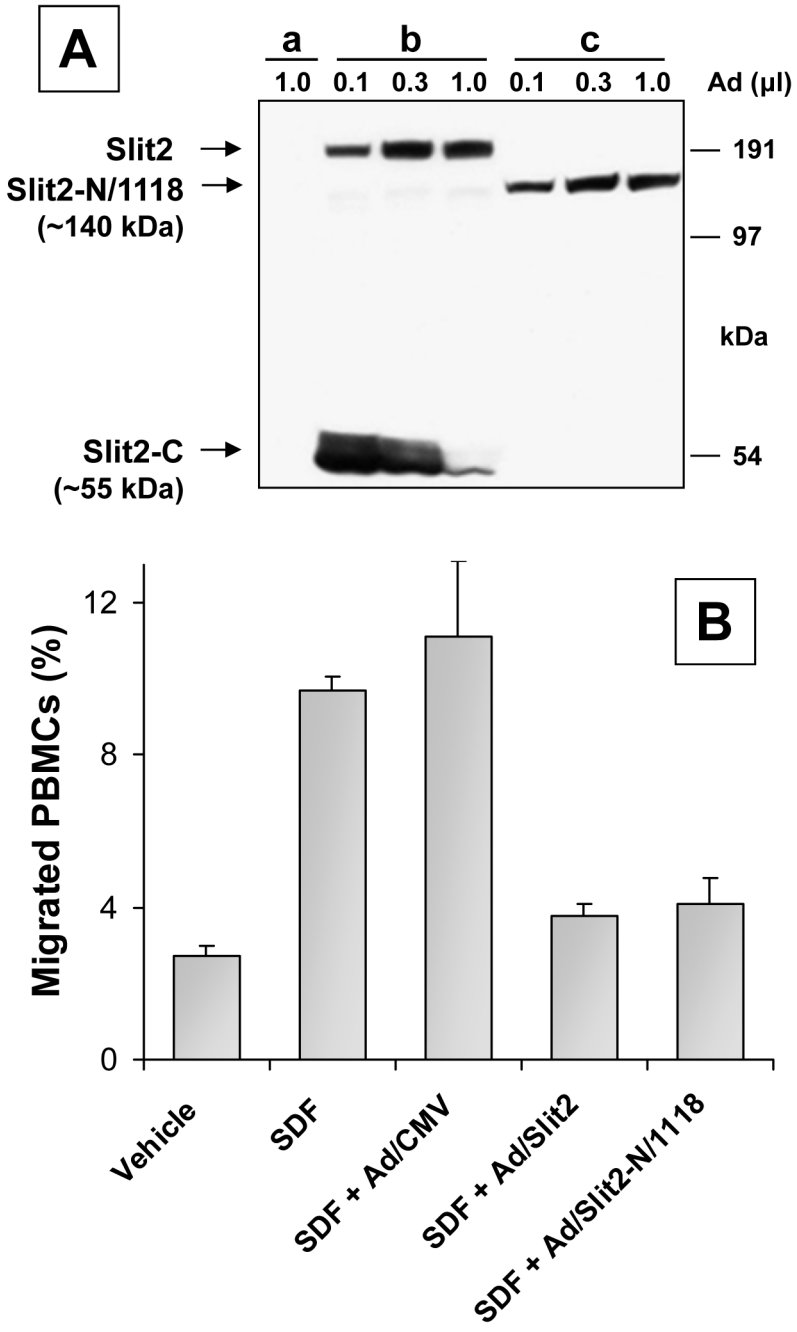

Figure 7. Expression and function of human Slit2 and Slit2-N/1118

A: Expression and identification of human Slit2 and Slit2-N/1118 by Western blotting. HEK-293 cells were infected with 3 concentrations (0.1, 0.3, and 1.0) of constructs bearing V5 tags at their C-terminal. Concentrated conditioned media (CM) from hAd/CMV/V5 (lane a), Ad/Slit2/V5 (lanes b), and Ad/Slit2-N/1118/V5 (lanes c) were analyzed by Western blotting using an anti-V5 Ab. Full-length Slit2 (~190 kDa) and its C-terminus fragment (~55 kDa) were detected in CM from Ad/Slit2/V5. CM from Ad/Slit2-N/1118/V5 shows only Slit2-N/1118, which was secreted and detected in the medium. **B. PBMC migration assay.** Rat PBMCs were seeded in standard migration chambers and incubated for 3 hours with

Author Manuscript Author Manuscript Author Manuscript Author Manuscript

vehicle or SDF-1 in the presence 20% CM from HEK-293 cells infected with adenoviral vectors for 48 hours. Migration of PBMCs was increased 3.5-fold by SDF-1. CM from Ad/Slit2/V5 and Ad/Slit2-N/1118/V5 inhibited migration to control levels, whereas CM from cells infected with the control vector (Ad/CMV/V5) did not prevent SDF-1-mediated PBMC migration. A representative experiment (n=3 migration inserts) is shown, 2 additional experiments showed similar results.

Author Manuscript Author Manuscript Author Manuscript Author Manuscript

Table 1

Primer Pairs of Rat and Human Slit and Robo Genes for Real-Time PCR

Gene	Acc. No.	Forward Primer	Reverse Primer	PL (bp)
rSlit1	NM_022953	AAGTGTGATCCCTGCTTGTC	TATGCCATCCACACAGACAC	299
rSlit2	AF141386	GTGCGTCTGGTGTGAATGAG	ATGCTCCTGGTGCAACTGTG	210
rSlit-3	NM_031321	TTCAACGGGCTAAGGTCACTCC	GCACTTGGCCACGATGTTAATG	297
rRobo1	NM_022188	GAAGCATCAGCCACTTTGACAG	GGTCCGCAATCACATCAGTAAC	337
rRobo2	XM_213677	ACCCCCAGTTCCACCATTAGG	GCAGAGCCCCATCCATTTACC	204
rRobo3	XM_236056	GGGGGTGATCGCAACAGCAGTAT	GTAGCAGTCCCCGGAACATCACAG	172
rRobo4	NM_181375	GGCCCCACCTCCTGCTGAAAAC	GGACGGCACCACTGGCAATGACT	329
rICAM-1	NM_012967	CCCGGAGGATCACAAACGAC	ATAGGCAGCGGGACACCATC	243

Acc. No.: accession number; PL (bp): product length (base pairs)